IAC-25,B2,IP,46,x100732

Satellite-based entanglement distribution for global quantum networks

Philipp Kleinpaß a*, Jaspar Meister b, Davide Orsucci a

Abstract

Finding a realistic and efficient scheme that allows for the distribution of entanglement at global scales constitutes a challenging task with a satisfactory solution yet to be found. Due to the exponential losses experienced in optical fibers and the absence of a direct line-of-sight between opposite sides of Earth, employing a quantum repeater chain will likely be inevitable to achieve this task. Long-distance terrestrial fiber connections would require a huge number of intermediate repeater nodes and is further hindered by inaccessible terrain, so that quantum repeaters realized via free-space optical links between satellites constitute a promising alternative. These, however, introduce their own set of challenges, such as the dynamic behaviour of the satellites in orbit and a high baseline of losses due to the satellite-to-ground connection. In this work, we discuss the general scaling properties of free-space optical quantum repeaters and combine them with the geometric constraints imposed by satellite connections to propose and assess a two-node two-satellite quantum repeater architecture that allows entanglement distribution at truly global scales whilst also being able to adaptively be used as a one-node one-satellite repeater to efficiently cover shorter distances. We provide an analysis of the connection time and the effective transmission and show that two MEO satellites are sufficient to distribute entanglement between ground stations with arbitrary distances inside the orbital plane. We deem our architecture as one of the most promising in terms of performance, connection distance and flexibility whilst using only two satellites, alleviating the extreme technical challenge of realizing a quantum repeater constellation.

1. Introduction

Entanglement constitutes one of the most powerful resources of quantum mechanics, yet its distribution at global scales imposes major technological challenges, with the record distance of 1120 km established by the Micius satellite mission [1]. Fundamental principles of quantum mechanics prohibit a direct signal amplification and the exponential losses experienced by photons in optical fibers render direct long-distance entanglement distribution via terrestrial networks an infeasible task. Employing free-space optical (FSO) channels supported by satellites substitutes the exponential losses for a polynomial decay, yielding a much better scaling with the distance but introducing additional challenges due to the dynamic conditions experienced by optical satellite links.

The concept of quantum repeaters was introduced to counteract the large losses experienced in long-distance entanglement distribution [2]. Here, a number of intermediate nodes is employed to divide the total distance into

shorter channels that independently distribute entanglement and, upon success, store the entangled photons in quantum memories located at each node until all channels succeeded. Afterwards, each node performs a Bell-State measurement (BSM), transforming the entanglement generated in the individual channels to an entangled state between the two outermost ones, thereby generating endto-end entanglement [3]. In optical fibers, this procedure yields an exponential gain of the transmission with the distance, however, with respect to an already exponentially damped channel. Therefore, many intermediate nodes are necessary to achieve a sufficiently good performance, posing a major technological challenge especially considering terrestrial obstructions such as mountains and oceans [4]. For FSO channels, instead, the gain is constant in the distance and quickly saturates in the number of nodes, thus a considerable advantage is only expected for a very small number of nodes. Therefore, previous works on satellitebased quantum repeaters have mostly studied one-node re-

IAC-25,B2,IP,46,x100732 Page 1 of 7

^a German Aerospace Center (DLR), Institute of Communications and Navigation, Münchener Str. 20, 82234 Weßling E-mail: philipp.kleinpass@dlr.de

^b German Aerospace Center (DLR), Institute for Satellite Geodesy and Inertial Sensing, Callinstrasse 30b, 30167 Hannover

^{*} Corresponding author

peater configurations which, however, exhibit pronounced disadvantages in terms of performance, requirements and flexibility, making the tremendous effort of realizing a space-based quantum repeater node hard to justify [5–8]. In this work, we systematically analyze the gain achieved by an FSO quantum repeater chain to formulate some simple criteria that guide us in the selection of a promising architecture (section 2), before combining them with the geometric constraints introduced by the satellite channels (section 3) to select and analyze a specific medium earth orbit (MEO) configuration that can adaptively operate as two-node two-satellite or one-node one-satellite quantum repeater (section 4 and section 5).

2. Scaling and Gain

A common architecture considered for the realization of an N-node repeater chain is to further subdivide each of the N + 1 channels by introducing another intermediate node that does not contain quantum memories and solely serves to distribute the entanglement over the corresponding channel, as depicted in fig. 1. This may be either a source, which generates and transmits two entangled photons, or a receiver, which performs BSMs between two photons received from the adjacent repeater nodes. In the both cases, for a successful generation of entanglement across the n-th channel both photons need to reach their destination nodes through the two sub-channels, with the corresponding transmissions denoted as $\eta_{n,1}$ and $\eta_{n,2}$. For a fiber-based repeater chain, the losses scale exponentially with the distance according to some absorption parameter α , thus the subdivision of a channel with length d_n into two sub-channels with lengths $d_{n,1} + d_{n,2} = d_n$ does not change the total transmission:

$$\eta_{n,1} \, \eta_{n,2} = e^{-\alpha (d_{n,1} + d_{n,2})} = e^{-\alpha d_n} = \eta_n \,.$$
(1)

For FSO channels, however, the losses scale quadratically with the distance, if the receiver is in the far field of the transmitter. Thus, assuming equal effective aperture areas A and wavelenghts λ , the transmission when sub-dividing the channel reads

$$\eta_{n,1} \, \eta_{n,2} = \frac{A^4}{(\lambda^2 d_{n,1} d_{n,2})^2} \ll \frac{A^2}{\lambda^2 d_n^2} = \eta_n, \quad (2)$$

if the distances $d_{n,1}$ and $d_{n,2}$ become sufficiently large. Therefore, we arrive at

Conclusion 1: Subdividing long-distance free-space optical channels between repeater nodes should be avoided whenever possible.

Since, statistically, once the worst channel successfully distributes entanglement, all other channels have already succeeded, the performance of the whole repeater chain is dominated by the worst channel. Therefore, optimal performance is achieved for symmetric channels $\eta_n \approx \eta_{n+1}$ and the total distance D should be divided into N+1 equal channels of distance D/(N+1). After each channel succeeded, a successful end-to-end entanglement generation is achieved when each node successfully performs a BSM between two photons stored in the memories corresponding to the adjacent channels. If each node has an individual probability of p to perform a successful BSM, then the total success probability P of an end-to-end entanglement generation is given by

$$\underbrace{P(N) = \frac{p^N 16A^4}{\lambda^4 D^4} (N+1)^4}_{\text{with subdivision}}, \quad \underbrace{P(N) = \frac{p^N A^2}{\lambda^2 D^2} (N+1)^2}_{\text{without subdivision}},$$
(3)

where subdivision refers to the case of further subdividing each channel into two equally-distant sub-channels as discussed above. These expressions increase polynomially in the amount of repeater nodes, but are exponentially suppressed by the individual BSM success probabilities. The gain in performance expected when moving from N-1 to N repeater nodes g(N) = P(N)/P(N-1) reads

$$\underbrace{g(N) = p \frac{(N+1)^4}{N^4}}_{\text{with subdivision}}, \quad \underbrace{g(N) = p \frac{(N+1)^2}{N^2}}_{\text{without subdivision}}. \quad (4)$$

For an N-node repeater to make sense, $g(N) \ge 1$ is a necessary condition. Furthermore, for any p < 1, there is an optimal number of nodes N satisfying $g(N+1) \le 1$, i.e. introducing an additional node decreases the end-to-end success probability. This leads to the optimal number of nodes

$$N_{\text{opt}} = \left\lfloor \frac{p^{1/4}}{1 - p^{1/4}} \right\rfloor, \qquad N_{\text{opt}} = \left\lfloor \frac{p^{1/2}}{1 - p^{1/2}} \right\rfloor. \tag{5}$$
with subdivision
without subdivision

As depicted in fig. 2, however, the gain of introducing an additional repeater node saturates quickly even for p=1, where formally $N_{\rm opt} \to \infty$. Since each additional repeater node also introduces a huge technical and financial overhead we arrive at

Conclusion 2: In practice, for terrestrial distances, the optimum number of repeater nodes in a free-space optical channel will likely not exceed two.

IAC-25,B2,IP,46,x100732 Page 2 of 7

Copyright ©2025 by Deutsches Zentrum für Luft- und Raumfahrt e.V. (DLR). Published by the IAF, with permission and released to the IAF to publish in all forms.

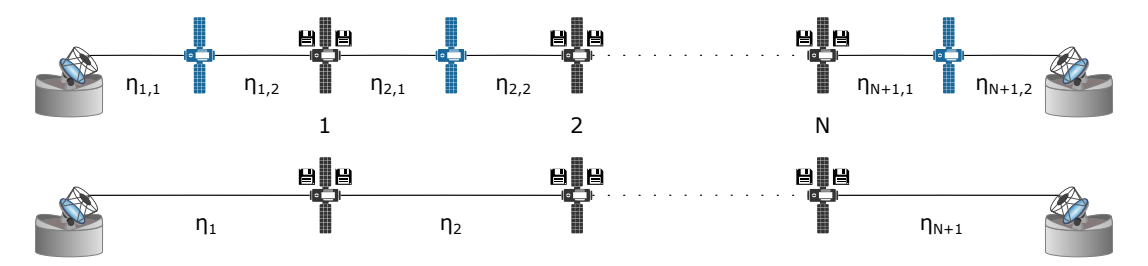


Fig. 1: *Upper row:* N-node satellite-based repeater chain where each channel is subdivided by an additional satellite without quantum memories that serves to distribute entanglement between the adjacent nodes. *Lower row:* N-node repeater chain with every satellite acting as a repeater node and no further subdivision.

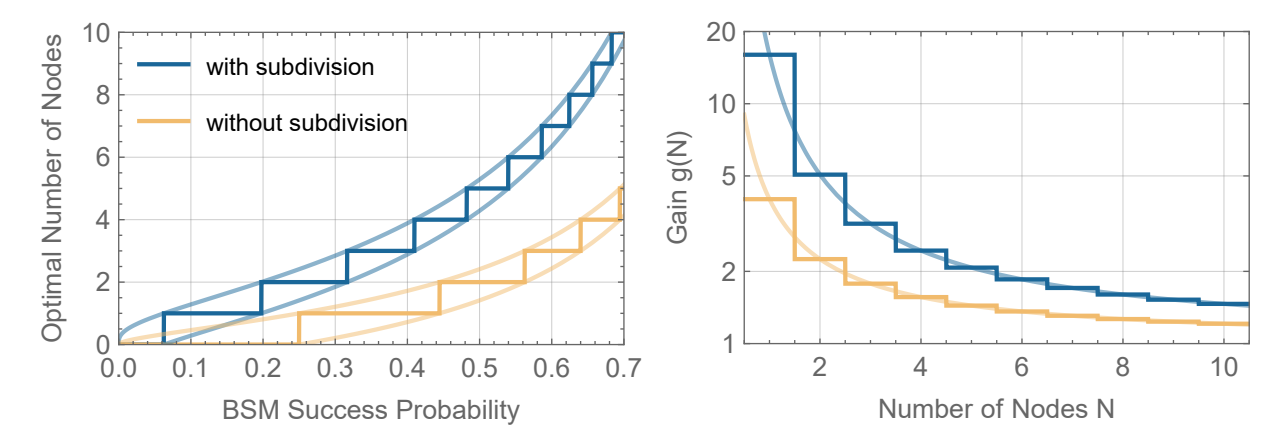


Fig. 2: Left: Optimal number of nodes depending on the individual BSM success probabilities p. Right: Maximum achievable gain in performance when moving from N-1 to N nodes (p=1).

3. Geometric Constraints

When considering geometric constraints faced by FSO satellite channels, the conclusions of the previous section are not that straight forward to apply. For instance, when connecting two optical ground stations (OGS) on distant points on Earth, even without introducing any repeater node the channel trivially needs to be subdivided at least once since there is no direct line-of-sight between both OGS. Since, according to eq. (A3), a single satellite in Low Earth Orbit (LEO) can only cover a very limited distance up to a few thousand kilometers, a direct distribution scheme without any repeater nodes would likely yield the highest performance from a geosynchronous orbit (GSO), where distances roughly up to one third of Earth's circumference could be connected. Due to the subdivision of the channel, however, this results in rather low entanglement generation rates that might prove insufficient for most practical applications.

A natural extension would therefore be to employ a GSO satellite as a one-node repeater, since this requires no fur-

ther subdivision and is expected to yield a quadratic increase in performance. As mentioned before, however, the entanglement distribution is limited to a specific area around its zenith and no global connection can be achieved. To increase the communication range to global distances (half of Earth's circumference) via one-node repeater architectures, additional satellites have to be introduced to overcome line-of-sight limitations. The problem that arises is that in a one-node two-satellite architecture, there is a drastic asymmetry in the channel losses between the endnodes and the repeater-node, which drastically lowers the performance due to the scaling property of the repeaterchain according to the worst channel. Therefore, to ensure roughly equal losses between both end-nodes and the repeater, a one-node three-satellite architecture would be required. Here, the channels between the end-nodes and the repeater node are both subdivided by an additional satellite and again, as discussed in the previous section, this leads to a drastic decrease in performance.

To satisfy the conclusions of the previous section while in-

IAC-25,B2,IP,46,x100732 Page 3 of 7

corporating the geometric constraints imposed by the satellite links, we propose a two-satellite two-node repeater constellation that allows for global connectivity whilst avoiding any channel subdivisions between repeater/end-nodes.

4. Two-Node Two-Satellite Repeater Orbit

In order to connect two OGS on opposite sides of Earth, we require that at some point in time t = 0 each ground station has a direct line-of-sight to one of the satellites, with positive and equal elevation angles $\varepsilon_0 = \varepsilon(t = 0)$, measured w.r.t. the tangential plane at the respective point and facing away from Earth, and a direct line-of-sight between the satellites. Restricting ourselves to circular orbits, we can derive the radius of the orbit by considering the Earth as a circle with radius $R_{\rm E}$ in the center of our coordinate system, with the ground stations being located at the coordinates $(x, y) = (0, \pm R_E)$. The lineof-sight from the respective ground stations corresponding to a simultaneous elevation of ε_0 can then be represented as $y = \pm (R_{\rm E} + x \tan \varepsilon_0)$. The closest we can place the two satellites on those lines whilst establishing a direct line-of-sight between them is at $x = R_E$, corresponding to the coordinates $(R_{\rm E}, \pm R_{\rm E}(1 + \tan \varepsilon_0))$. The radius of the corresponding orbit is simply given by the distance of those points from the center of the coordinate system: $R_{\rm O}^2 = x^2 + y^2$, leading to

$$R_{\rm O} = R_{\rm E} \sqrt{1 + (1 + \tan \varepsilon_0)^2}$$
, (6)

with the orbit height h obtained by subtracting the radius of the Earth

$$h = R_{\rm E} \left(\sqrt{1 + (1 + \tan \varepsilon_0)^2} - 1 \right)$$
 (7)

and the angle between the satellites given as

$$\delta = 2\arctan(1 + \tan \varepsilon_0). \tag{8}$$

While higher orbits lead to longer connection times, the increased link distances lead to higher channel losses. To keep the links as short as possible whilst enabling global connectivity, a MEO orbit with an altitude of $h \approx R_{\rm E}$, right outside the inner Van Allen radiation belt [9] constitutes a reasonable compromise, as depicted in fig. 3.

Since we consider a circular orbit, the intersatellite distance will remain constant and amounts to $D_{\rm IS} \approx 22\,000\,{\rm km}$, with the angle between both satellites measured from the center of Earth amounting to $\delta=120^{\circ}$. Due to the dynamic behaviour of the satellites following their orbits, the distance to the respective ground station will be determined by the instantaneous elevation $\varepsilon(t)$

$$D_{\rm OGS}(t) = R_{\rm E} \left(\sqrt{4 - \cos^2 \varepsilon(t)} - \sin \varepsilon(t) \right) \,. \tag{9}$$

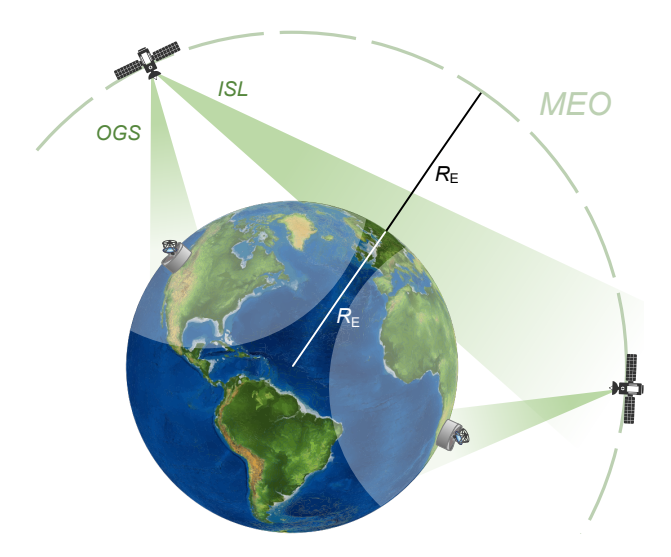


Fig. 3: Two-node two-satellite quantum repeater constellation. The MEO orbit with an altitude of approximately $R_{\rm E}$ maximizes the connection time for opposite points on earth whilst minimizing the inter-satellite distance for maximum performance.

It reaches its maximum value at the point in time where $\varepsilon(t) = 0^{\circ}$, corresponding to $D_{\text{OGS}} = \sqrt{3}R_{\text{E}} \approx 11\,000\,\text{km}$.

5. Results

As discussed in section 2, at each point in time the end-to-end performance of the repeater-chain is governed by the channel with the worst instantaneous transmission $\underline{\eta}(t)$. Since, for the two-node two-satellite constellation, the inter-satellite distance is at least twice as large as the distance to ground, even without explicitly modelling additional effects such as turbulence and absorption in the satellite-to-ground channels, the instantaneous rates will most likely be limited by the transmission of the intersatellite channel

$$\underline{\eta(t)} = \begin{cases} \frac{A_{\text{SAT}}^2}{\lambda^2 D_{\text{ISL}}^2} & \text{for } -\frac{T}{2} \le t \le \frac{T}{2}, \\ 0 & \text{else,} \end{cases}$$
(10)

where the satellite-to-ground channels determine the simultaneous connection time to both ground stations T, the effective radius of satellite and ground station aperture is given as $r_{\rm SAT}=0.25\,\mathrm{m}$ and $r_{\rm OGS}=0.5\,\mathrm{m}$, respectively, and connected to the corresponding aperture size according to $A=\pi r^2$, and a wavelength of $\lambda=1550\,\mathrm{nm}$ is assumed. For a versatile usage of the satellites, ideally we should be able to connect ground-stations at arbitrary distances.

IAC-25,B2,IP.46,x100732 Page 4 of 7

Copyright ©2025 by Deutsches Zentrum für Luft- und Raumfahrt e.V. (DLR). Published by the IAF, with permission and released to the IAF to publish in all forms.

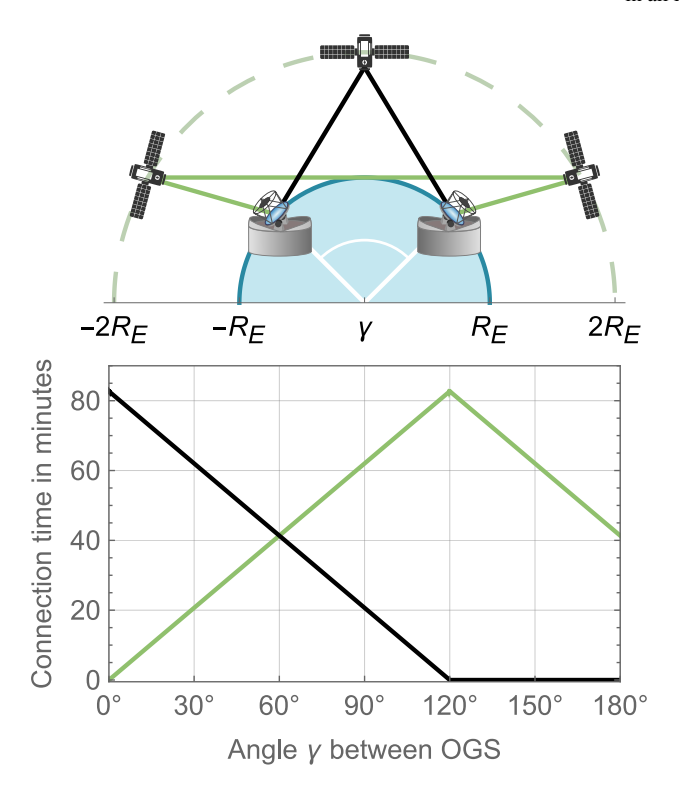


Fig. 4: Maximum simultaneous connection time of two ground stations separated by an angle of γ w.r.t. the center of Earth when considering either each ground station connecting to one of the satellites (green) or both ground stations connecting to the same satellite (black).

Therefore, we vary the positions of the OGS in the orbital plane by introducing the angle γ between both ground stations measured from the center of Earth. For the simultaneous two-satellite connection, the lowest connection time is present when both OGS are placed close to each other, i.e. for $\gamma \to 0^{\circ}$. In this case, however, instead of using the simultaneous two-satellite connection, the distance between both ground stations is sufficiently small to use each satellite as an individual one-node repeater distributing entanglement via a simultaneous line-of-sight to both OGS. In fig. 4, the total simultaneous connection time T for one satellite pass is depicted for different angles between the ground stations and when using either a two-node twosatellite connection, where each of the satellites communicates to one ground station, and a one-node one-satellite connection, where one satellite connects to both ground stations at once. If the ground stations are directly on top of each other, the simultaneous connection time to a single satellite is maximized while the two-satellite communication time is zero. The further the ground stations move away from each other, the smaller the single-satellite and the larger the two-satellite communication times become, until they reach equality at an angle of $\gamma=60^\circ$. This trend continues up to an angle of $\gamma=120^\circ$, where no simultaneous line-of-sight between one satellite and both ground stations can be established but, instead, the two-satellite communication time is maximized. The time evolution of the transmission for the corresponding satellite-to-ground channels

$$\eta_{\rm OGS}(t) = \begin{cases} \frac{A_{\rm OGS}A_{\rm SAT}}{\lambda^2 D_{\rm OGS}^2(t)} & \text{for} & -\frac{T}{2} \le t \le \frac{T}{2} ,\\ 0 & \text{else,} \end{cases}$$
(11)

is presented in fig. 5 for various values of γ . The origin of time is chosen at the point where both ground stations see the respective satellite at the same elevation and the shaded areas correspond to the maximum total communication time until the elevation at one of the ground stations reaches zero and the connection is lost.

As the simultaneous connection of both ground stations to one satellite does not require an inter-satellite link, the instantaneous entanglement distribution rate heavily depends on the elevation angle and the additional losses introduced by atmospheric effects. Since explicitly modelling the atmospheric channel is not within the scope of this work, we depict a range of additional losses determined by a parameter $\eta_{\rm ATM} \in [0.1,1]$, such that, for the one-node one-satellite configuration, the effective simultaneous transmission is given as

$$\eta(t) = \eta_{\text{ATM}} \eta_{\text{OGS}}(t).$$
(12)

Since, at each point in time, the instantaneous transmission is roughly proportional to the entanglement distribution rate, the total amount of entanglement distributed over one (simultaneous) satellite pass of duration T is proportional to the time-integrated transmission

$$\mathcal{T} = \int_{T} \underline{\eta(t)} dt, \qquad (13)$$

yielding a convenient measure to compare the one-satellite to the two-satellite configuration. The results are presented in fig. 6 and given in decibel-seconds $(10\log_{10}\mathcal{T})$. Depending on the additional losses in the satellite-to-ground channel, the two-satellite connection can outperform the one-satellite connection for angles of $\gamma \geq 80^\circ$. Note however, that the two-satellite connection features an additional repeater node which introduces additional losses due to effects like non-unit BSM success probabilities (p < 1) and decoherence due to increased communication times that are not considered here.

IAC-25,B2,IP,46,x100732 Page 5 of 7

Copyright ©2025 by Deutsches Zentrum für Luft- und Raumfahrt e.V. (DLR). Published by the IAF, with permission and released to the IAF to publish in all forms.

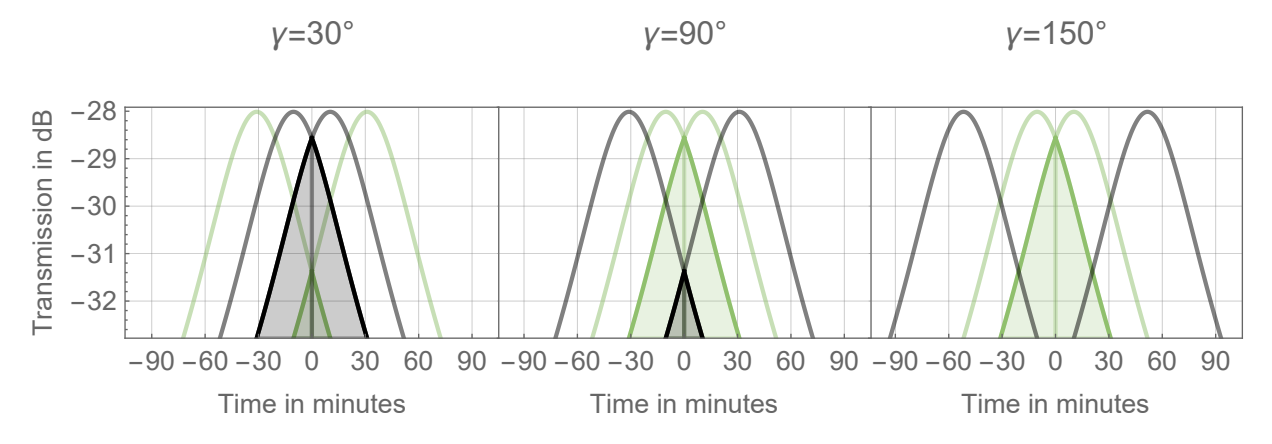


Fig. 5: Transmission over time when connecting two optical ground stations with one MEO satellite acting as a one-node repeater (black), and two MEO satellites acting as a two-node repeater (green), with the two curves corresponding to the two ground stations and the overlap between them representing the joint connection time. The origin of time is chosen at the point where both ground stations measure the same elevation angle to the satellite.

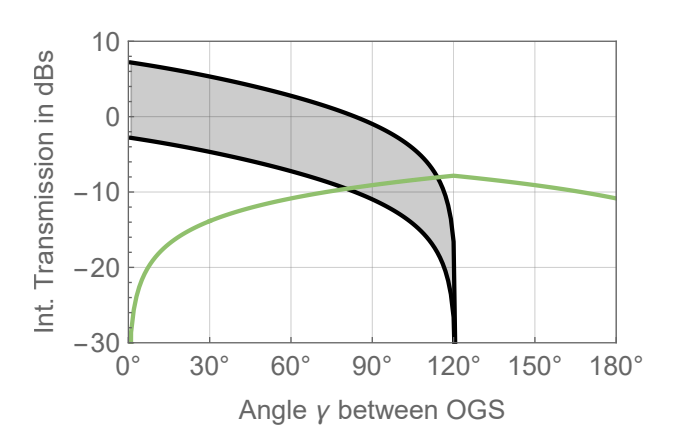


Fig. 6: Time-integrated effective transmission over the whole satellite pass in decibel-seconds when changing the angle γ between the ground stations. The black curve represents the one-node one-satellite repeater with the effective transmission at each point in time given by the minimum transmission of the two satellite-to-ground channels. Since atmospheric effects are not explicitly modelled, a range of up to 10 dB of additional losses is depicted. The green curve represents the two-node two-satellite repeater, where the instantaneous transmission is governed by the inter-satellite channel and the connection time is determined by the overlap of the two satellite-to-ground connections.

6. Conclusion and Discussion

In this work, we proposed and discussed an architecture for a two-satellite quantum repeater constellation that allows for global entanglement distribution by being able to simultaneously connect two ground stations on opposite sides of Earth. We proposed this architecture based on the observation that a quantum repeater over free-space optical channels only yields a reasonable gain for a very small number of repeater nodes, the observation that subdividing the channels between repeater nodes by introducing additional satellites leads to a drastic increase of losses and the fact that the performance of a quantum repeater chain is maximized when all channels exhibit roughly equal losses. Since global coverage requires the use of at least two satellites, this led us to the conclusion that a two-node twosatellite quantum repeater constellation is likely optimal for this task, given that it features a symmetric setup without introducing additional satellites and has the flexibility to act as a one-node one-satellite repeater to cover shorter distances. A natural choice of orbit that was analyzed is a MEO orbit with an altitude roughly amounting to the radius of Earth, since this is the lowest orbit that allows for global coverage whilst being outside of the Van-Allen radiation belt. Considering only the quadratic losses due to the free-space optical signal propagation, we assessed the performance achieved in this configuration for arbitrary distances between the two ground stations within the orbital plane and estimated the distance at which it becomes beneficial to switch from the one-node one-satellite configuration to the two-node two-satellite configuration. We believe that this architecture is a promising contender

IAC-25,B2,IP,46,x100732 Page 6 of 7 for truly global satellite-based entanglement distribution, since its ability to provide efficient global coverage with only a few satellites adds minimum overhead to the outstanding technical challenges faced by realizing a global repeater chain. To substantiate this claim, future work will be concerned with a more detailed quantitative analysis of the expected performance, adding many crucial details regarding the quantum memories, the repeater protocol, the atmospheric channels and the long-term performance of a suitable 3D satellite constellation.

Acknowledgements

This work was conducted in the framework of the DLR internal project *Robust Global Quantum Networks* (RoGlo-QuaN) and the ESA-funded project *Satellite-Distributed Quantum Computing* (Sat-DQC) with the contract number 4000147454.

Appendix A. Circular Orbits

Considering an optical ground station inside the orbital plane of a perfectly circular orbit with altitude h, the relation between the instantaneous elevation $\varepsilon(t)$ and the corresponding distance between satellite and OGS $D_{\rm OGS}(t)$ reads

$$\sin \varepsilon(t) = \frac{h^2 + 2hR_{\rm E} - D_{\rm OGS}^2(t)}{2D_{\rm OGS}(t)R_{\rm E}} \,. \tag{A1} \label{eq:alpha}$$

To obtain the temporal evolution of these quantities, we need to connect them to the angle β measured between the satellite and the OGS from the center of Earth

$$\cos\beta(t) = \frac{R_{\rm E} + D_{\rm OGS}(t)\sin\varepsilon(t)}{R_{\rm E} + h} \,. \tag{A2} \label{eq:A2}$$

Due to the circular nature of the orbit, the angular velocity of this angle is constant, i.e. $\beta(t) = \omega t$ with $\omega = \sqrt{GM_{\rm E}/(h+R_{\rm E})^3}$. Thus, eliminating $D_{\rm OGS}(t)$ from the above formulas we can express the temporal evolution of the elevation angle as

$$\sin \varepsilon(t) = \frac{(R_{\rm E}+h)\cos(\omega t) - R_{\rm E}}{\sqrt{h^2 + 2hR_{\rm E} - 2R_{\rm E}\left((R_{\rm E}+h)\cos(\omega t) - R_{\rm E}\right)}}\,, \eqno(A3)$$

up to a proper restriction to the interval $\epsilon(t) \in [0^{\circ}, 90^{\circ}]$. Since both eq. (A1) and eq. (A2) only exhibit an implicit time dependence, we can rephrase the distance and satellite-OGS angle as functions of the elevation angle $D_{\text{OGS}}(\varepsilon(t))$ and $\beta(\varepsilon(t))$. After eliminating the distance, we can use this to compute the length S of the arc on

the surface of Earth between two points that observe the satellite at an elevation of $\underline{\varepsilon}$ according to

$$S = 2\beta(\varepsilon)R_{\rm E}$$
, (A4)

corresponding to the maximum distance between two OGS to feature a simultaneous line-of-sight above some minimum elevation ε .

References

- [1] J. Yin, Y. H. Li, S. K. Liao, and et al. Entanglement-based secure quantum cryptography over 1,120 kilometres. *Nature*, 582:501–505, 2020.
- [2] H.-J. Briegel, W. Dür, J. I. Cirac, and P. Zoller. Quantum repeaters: The role of imperfect local operations in quantum communication. *Phys. Rev. Lett.*, 81:5932–5935, Dec 1998.
- [3] Michael A. Nielsen and Isaac L. Chuang. *Quantum Computation and Quantum Information*. Cambridge University Press, Cambridge; New York, 10th anniversary edition edition, 2010.
- [4] Kosuke Fukui, Rafael N Alexander, and Peter van Loock. All-optical long-distance quantum communication with Gottesman-Kitaev-Preskill qubits. *Physical Review Research*, 3(3):033118, 2021.
- [5] M. Gündoğan, J. S. Sidhu, V. Henderson, and et al. Proposal for space-borne quantum memories for global quantum networking. *npj Quantum Information*, 7:128, 2021.
- [6] J. Wallnöfer, F. Hahn, M. Gündoğan, et al. Simulating quantum repeater strategies for multiple satellites. *Communications Physics*, 5:169, 2022.
- [7] Mustafa Gündoğan, Jasminder S. Sidhu, Markus Krutzik, and Daniel K. L. Oi. Time-delayed single satellite quantum repeater node for global quantum communications. *Optica Quantum*, 2(3):140–147, Jun 2024.
- [8] Jaspar Meister, Philipp Kleinpaß, and Davide Orsucci. Simulation of satellite and optical link dynamics in a quantum repeater constellation. EPJ Quantum Technol., 12, 2025.
- [9] J. A. Van Allen, G. H. Ludwig, E. C. Ray, and C. E. McIlwain. Observation of high intensity radiation by satellites 1958 alpha and gamma. *Journal of Jet Propulsion*, 28(9):588–592, 1958.

IAC-25,B2,IP.46,x100732 Page 7 of 7